Supporting Information

Construction of $Ti_3C_2T_x$ MXene wrapped urchin-like $CuCo_2S_4$ microspheres for high-performance asymmetric supercapacitor

Xiaobo Chen [a *], Huiran Ge [a], Wen Yang [b], Peizhi Yang [b *]

a School of Physics and Electronic Engineering, Jiangsu Intelligent Optoelectronic Device and Measurement and Control Engineering Research Center, Yancheng Teachers University, Yancheng, 224051, PR China

b Key Laboratory of Education Ministry for Advance Technique and Preparation of Renewable Energy Materials, Solar Energy Research Institute, Yunnan Normal University, Kunming 650500, PR China

[*] E-mail addresses: chenxbok@126.com (X. Chen), pzhyang@hotmail.com (P. Yang).

Experimental details

Preparation of Few-layered $Ti_3C_2T_x$ MXene

$Ti_3C_2T_x$ MXene was synthesized via selective etching of Al layer from Ti_3AlC_2 MAX phase precursor using a concentrated mixture of LiF and HCl, according to previous literature [1]. Briefly, 1 g of LiF powder was blended with 20 mL 9 M HCl solution followed by gradual addition of Ti_3AlC_2 powder (1.0 g). Subsequently, the mixture was kept at 35°C with magnetic stirring of 24 h to selective etching the Al layer. The resulting suspension was continuously rinsed numerous times with deionized (DI) water to adjust the pH≈6 at a centrifuge speed of 4500 rpm, and then dried in an oven.

In order to prepare the fewer layered $Ti_3C_2T_x$ nanosheets, 30 mL of dimethyl sulfoxide was mixed with 1 g of as-prepared multilayer MXene and stirred for 24 h. Then the DMSO inserted in m-MXene was centrifugation at 4000 rpm/min for 5 min and rinsed with DI water to remove the dimethyl sulfoxide from fewer layered $Ti_3C_2T_x$ nanosheets. The obtained product was dispersed in DI water and sonicated

for 6 h. Subsequently, the resulting supernatant was collected and named as $Ti_3C_2T_x$ MXene colloidal solution (the concentration is about 2 mg ml^{-1}), used for further fabrication.

Structural characterizations

The X-ray diffraction (XRD) patterns recorded using a SHIMADZU XRD-6100 instrument with Cu-Kα radiation. The X-ray photoelectron spectra (XPS) were collected by a Thermo ESCALAB 250 electron spectrometer with an X-ray source of Al Ka. The scanning electron microscopy (SEM) imaging was conducted by Zeiss Supra 35VP scanning electron microscope, and the transmission electron microscopy (TEM) and high-resolution TEM (HRTEM) imaging was conducted by JEOL-2010 transmission electron microscope with 200 kV accelerated voltage. The specific surface area (BET method) of the samples were determined by nitrogen (N_2) adsorption/desorption using an ASAP 2020 V3.01 G instrument. The electrical conductivity were recorded through a standard four-point probe instrument (Cmt-sr1000n).

Electrochemical measurements

In this experiment, an active material ($CuCo_2S_4$, MXene/$CuCo_2S_4$), Poly(vinylidene fluoride) (PVDF, HSV900) and acetylene black with mass ratio of 8: 1: 1 were directly loaded on carbon fiber cloth and used as a working electrode. The loading mass of the active materials was weighted to be approximately 5 mg cm^{-2}.

In order to better interpretate the electrochemical behavior of the pure MXene in KOH electrolyte at potential ranges of 0–0.6 V, the free-standing MXene (1 cm^2; 5 mg/cm^2) with self-supported structure was directly used as the electrode.

All electrochemical tests were carried out on a CHI660E electrochemical workstation with the Ni foam carrying active material as the working electrode, Pt wire as the counter electrode was, and AgCl/Ag as the reference electrode. Besides, the electrolysis was 3 M KOH aqueous solution (50 mL). The galvanostatic charge/discharge (GCD) test and cycling test were conducted using a LAND battery program-control test system (CT2001A).

Fabrication of asymmetric supercapacitor device

Commercial activated carbon (AC) was used to prepare the negative electrodes as follows: AC powder, carbon black and PVDF were mixed in a ratio of 8:1:1 to obtain the electrode slurry. Then, the slurry was coated on carbon fiber cloth substrate and dried overnight at 80 °C in a vacuum oven. The solid-state asymmetric supercapacitor (ASC) device was built by utilizing Ti_3C_2 MXene/$CuCo_2S_4$ nanohybrid and activated carbon (AC) as cathode (positive) and anode (negative electrode) materials, respectively, gel electrolyte, and a separator (Whatman 42 paper). Before assembling the ASC device, the poly (vinyl alcohol) (PVA; Mw = 130 000)/KOH gel electrolyte (PVA/KOH) was prepared using the method as follows : 7.9 g of KOH and 6.0 g of PVA powder were mixed with 60 mL of DI water. Then, the whole mixture was stirred vigorously at 90 °C for 1 h to obtain a clear solution. Accordingly, two electrodes (positive and negative) and filter paper were doused in gel electrolyte solution of PVA/KOH for 20 min [2]. Afterward, the two soaked electrodes were sandwiched using the soaked filter paper to construct the solid-state device (Ti_3C_2 MXene/$CuCo_2S_4$//AC), followed by drying at RT under vacuum for 18 h. Finally, the electrochemical measurements of the as obtained ASC device were performed in two-electrode configuration system. According to the principle of charge balance between the positive (MXene/$CuCo_2S_4$) and negative (AC) electrode, the mass ratio of MXene/$CuCo_2S_4$ to AC is determined to be 1:1.9.

The specific capacity C_s (C g^{-1}) of Ti_3C_2 MXene, $CuCo_2S_4$, MXene/$CuCo_2S_4$ electrodes is obtained from Equation (S1) [3].

$$C_s = I\Delta t/m \quad \text{(S1)}$$

where Δt (s) is the discharge time after IR drop, I (A) is the applied current, m (g) is the is the loading mass of active material.

To explore the reaction kinetics, we further analyzed the linear correlation of the peak current (i) and sweep rate (v) based on the following formula [4]:

$$i = a \times v^b \quad \text{(S2)}$$

where (a, b) are constants, and the log (v) slope versus log(i) indicates the b-value which provides fundamental data about the charge storage kinetics.

The contribution ratio of capacitive and diffusion to the total charge storage can be determined from the CV curves using to the following equation, in which, k_1v stands for the capacitive controlled current and $k_1v^{1/2}$ represents diffusion control process [5]:

$$i(\mathrm{V}) = k_1v + k_2v^{1/2} \quad \text{(S3)}$$

The specific capacity C_{device} (C g^{-1}), energy density E (Wh kg^{-1}) and power density P (W kg^{-1}) of asymmetric supercapacitors can be calculated from the Equation (S4-S6), respectively [6].

$$C_{\mathrm{device}} = I\Delta t/m \quad \text{(S4)}$$

$$E = \frac{\int_{t1}^{t2} IV_{(t)}dt}{m \times 3.6} \quad \text{(S5)}$$

$$P = 3600E/\Delta t \quad \text{(S6)}$$

where I (A) corresponds to the applied current, Δt (s) means the discharging time after IR drop, m (g) represents the total loading mass of active materials on both cathode and anode, t_1 (s) is the initial time after IR drop, t_2 (s) is the final time of discharge, and $\int V(t)\mathrm{d}t$ is the integrated area of discharge curves after IR drop.

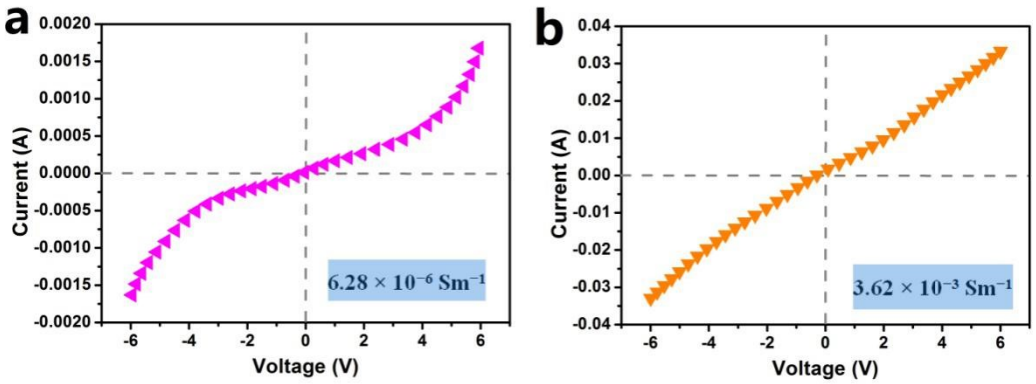

Fig. S1. Current-Voltage plots of (a) $CuCo_2S_4$ and (b) $CuCo_2S_4$/MXene-3.

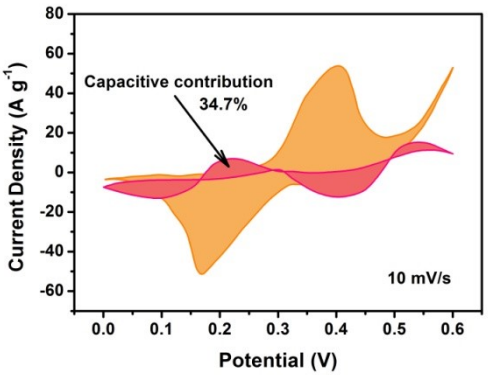

Fig. S2. Separation of diffusion and capacitive controlled currents of $CuCo_2S_4$/MXene-3 electrode at 10 mV s^{-1}.

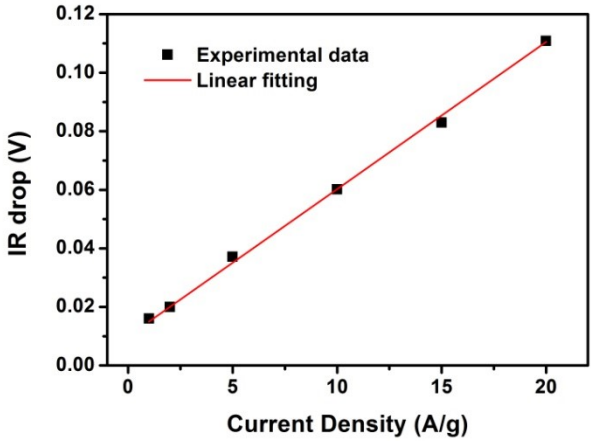

Fig. S3. Potential drop (IR drop) as a function of current density.

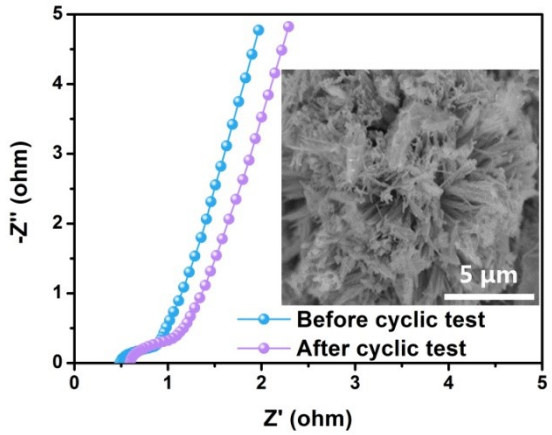

Fig. S4. Nyquist plots of the impedance spectra of $CuCo_2S_4$/MXene-3 before and after 10000 cycles. The inset is the SEM image of the $CuCo_2S_4$/MXene-3 electrode after cycling test.

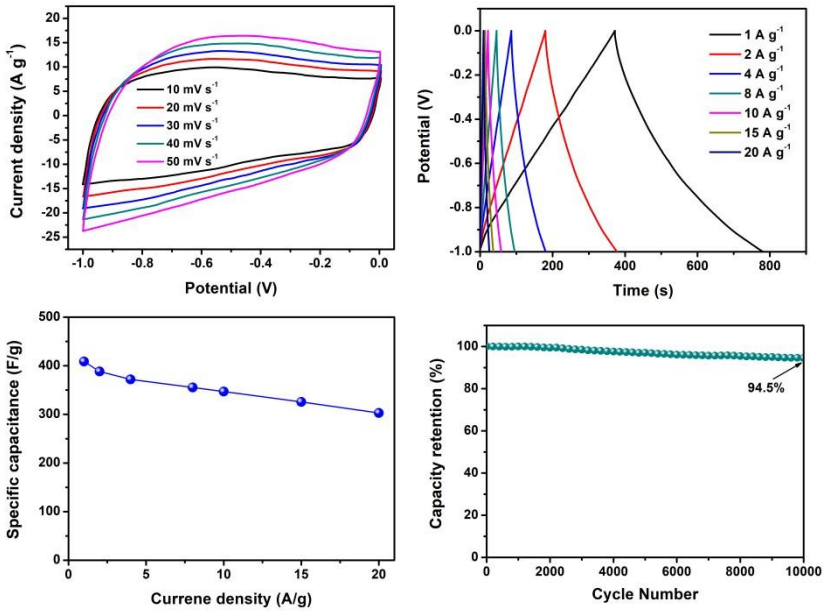

Fig. S5 (a) CV curves recorded at different scan rates and (b) GCD plots at different current densities of the AC electrode; (c) specific capacity values for AC electrode; (d) Cycling stability at 10 A g^{-1} for 10000 cycles.

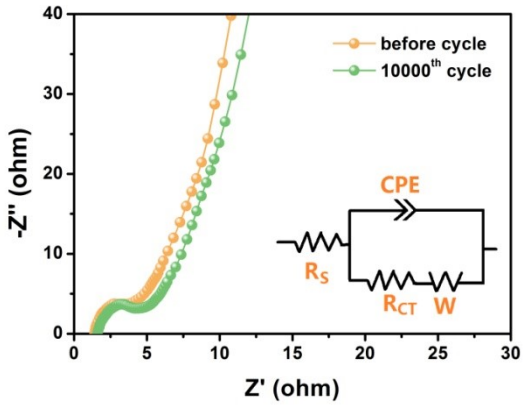

Fig. S6. Impedance spectra before and after 10000th cycle of $CuCo_2S_4$/MXene//AC device.

Table S1. Comparison of electrochemical performance of $CuCo_2S_4$/MXene-3 electrode with previous reports.

Materials	Electrolyte	Specific capacitance (C g^{-1})	Cycling performance	Ref.
$CuCo_2S_4$@$NiCo_2S_4$	3 M KOH	593.2 C g^{-1} at 1 A g^{-1}	100% after 5000 cycles at 8 A g^{-1}	[7]
$CuCo_2S_4$-45	2 M KOH	2879F g^{-1}, 1A g^{-1}	87.26% after 10000 cycles at 10 A g^{-1}	[8]
$CuCo_2S_4$	2 M KOH	515 F g^{-1} at 1 A g^{-1}	93.3% after 10000 cycles at 5 A g^{-1}	[9]
F-$CuCo_2S_{4-x}$	1 M KOH	2202.7 C g^{-1} at 1 A g^{-1}	96.7% after 5000 cycles at 20 A g^{-1}	[10]
$CuCo_2S_4$/CNTs-3.2%	2 M KOH	557.5 F g^{-1} at 1 A g^{-1}	\	[11]
$CuCo_2S_4$ nanoparticles	2 M KOH	1885.49 C g^{-1}/523.75 mA h g^{-1} at 2 A g^{-1}	98% after 6000 cycles at 10 A g^{-1}	[12]
$CuCo_2S_4$/Polyaniline	1 M Na_2SO_4	920 F g^{-1} at 1 A g^{-1}	96.29 % after 10,000 cycles at 10 A g^{-1}	[13]
$CuCo_2S_4$@NDG	6 M KOH	1839 F g^{-1} at 5 A g^{-1}	85.3% after 2000 cycles at 50 A g^{-1}	[14]
$CuCo_2S_4$/MXene-3	3 M KOH	1351.6 C g^{-1} at 1 A g^{-1}	95.2% after 10,000 cycles at 6 A g^{-1}	This work

Table S2. A comparison on the specific capacitance, specific energy, specific power and electrolyte of $CuCo_2S_4$/MXene//AC ACS with the previously reported ASCs devices.

Device	Specific capacity at current density	Specific energy (Wh kg^{-1})	Specific power (W kg^{-1})	Cycle Performance	Ref.
$CuCo_2S_4$/$CuCo_2O_4$-4//GA	90.4 F g^{-1} at 1 A g^{-1}	33.2	800	73% 10000 cycles	[15]
$CuCo_2S_4$-45//AC	231 F g^{-1} at 1 A g^{-1}	63.6	700	82.02% 10000 cycles	[8]
$CuCo_2S_4$//AC	112.4 F g^{-1} at 5 A g^{-1}	50.6	4600	99% 10000 cycles	[9]
$CuCo_2S_4$/NG//NG	150 F g^{-1} at 1 A g^{-1}	53.3	800	92.2% 4000 cycles	[16]
F-$CuCo_2S_{4-x}$//AC	224.0 C g^{-1} at 1 A g^{-1}	49.8	897.39	89.2% 10,000 cycles	[10]
$CuCo_2S_4$/CNTs-3.2%//AC	65.1F g^{-1} at 0.5A g^{-1}	23.2	402.7	85.7% 10,000 cycles	[11]
$CuCo_2S_4$@NDG//rGO	166 F g^{-1} at 1 A g^{-1}	58.4	797	97.5% 5000 cycles	[14]
$CuCo_2S_4$/MXene//AC	219.6 F g^{-1} at 1 A g^{-1}	78.1	800.7	95.9% 10,000 cycles	This work

References

[1] T.-Z. Shi, Y.-L. Feng, T. Peng, B.-G. Yuan, Sea urchin-shaped Fe_2O_3 coupled with 2D MXene nanosheets as negative electrode for high-performance asymmetric supercapacitors, Electrochim. Acta 381 (2021) 138245.

[2] P. Bandyopadhyay, X. Li, N. H. Kim, J. H. Lee, Graphitic carbon nitride modified graphene/NiAl layered double hydroxide and 3D functionalized graphene for solid-state asymmetric supercapacitors, Chem. Eng. J. 353 (2018) 824-838.

[3] R. Zhang, C. Lu, Z. Shi, T. Liu, T. Zhai, W. Zhou, Hexagonal phase NiS octahedrons co-modified by 0D-, 1D-, and 2D carbon materials for high-performance supercapacitor, Electrochim. Acta 311 (2019) 83-91.

[4] W. Lu, J. Shen, P. Zhang, Y. Zhong, Y. Hu, X. W. Lou, Construction of CoO/Co-Cu-S hierarchical tubular heterostructures for hybrid supercapacitors. Angewandte Chemie, 131

(2019) 15587-15593.

[5] K. A. Sree Raj, A. S. Shajahan, B. Chakraborty, C. S. Rout, Two-Dimensional Layered Metallic VSe_2/SWCNTs/rGO Based Ternary Hybrid Materials for High Performance Energy Storage Applications. Chem.-Eur. J. 26 (2020) 6662-6669.

[6] J. Sun, X. Du, R. Wu, Y. Zhang, C. Xu, H. Chen, Bundlelike $CuCo_2O_4$ microstructures assembled with ultrathin nanosheets as battery-type electrode materials for high-performance hybrid supercapacitors. ACS Appl. Energy Mater. 3 (2020) 8026-8037.

[7] L. Ma, T. Chen, S. Li, P. Gui, G. Fang, A 3D self-supported coralline-like $CuCo_2S_4$@$NiCo_2S_4$ core–shell nanostructure composite for high-performance solid-state asymmetrical supercapacitors. Nanotechnology 30 (2019) 255603.

[8] J. Jiang, Y. Chen, X. Hu, H. Cong, Q. Zhou, H. Rong, Y. Sun, S. Han, Designed synthesis of 2D multilayer $CuCo_2S_4$ nanomaterials for high-performance asymmetric supercapacitors. Vacuum, 182 (2020) 109698.

[9] S. Guo, W. Chen, M. Li, J. Wang, F. Liu, J. P. Cheng, Effect of reaction temperature on the amorphous-crystalline transition of copper cobalt sulfide for supercapacitors. Electrochim. Acta, 271 (2018) 498-506.

[10] L. Kang, C. Huang, J. Zhang, M. Zhang, N. Zhang, S. Liu, Y. Ye, C. Luo, Z. Gong,C. Wang, X. Zhou, X. Wu, S. C. Jun, Effect of fluorine doping and sulfur vacancies of $CuCo_2S_4$ on its electrochemical performance in supercapacitors. Chem. Eng. J., 390 (2020) 124643.

[11] H. Li, Z. Li, Z. Wu, M. Sun, S. Han, C. Cai, W. Shen, X.T. Liu, Y. Fu, Enhanced electrochemical performance of $CuCo_2S_4$/carbon nanotubes composite as electrode material for supercapacitors. J. Colloid Inter. Sci., 549 (2019) 105-113.

[12] M. Dakshana, S. Meyvel, M. Malarvizhi, P. Sathya, R. Ramesh, S. Prabhu, M. Silambarasan, Facile synthesis of $CuCo_2S_4$ nanoparticles as a faradaic electrode for high performance supercapacitor applications. Vacuum, 174 (2020) 109218.

[13] M. Abuali, N. Arsalani, I. Ahadzadeh, Investigation of electrochemical performance of a new nanocomposite: $CuCo_2S_4$/Polyaniline on carbon cloth. J. Energy Storage, 32 (2020) 101694.

[14] L. Chen, R. Lin, C. Yan, Nitrogen-doped double-layer graphite supported $CuCo_2S_4$ electrode for high-performance asymmetric supercapacitors. Mater. Lett., 235 (2019) 6-10.

[15] X. Xu, Y. Liu, P. Dong, P.M. Ajayan, J. Shen, M. Ye, Mesostructured $CuCo_2S_4$/$CuCo_2O_4$ nanoflowers as advanced electrodes for asymmetric supercapacitors, J. Power Sources, 400 (2018) 96-103.

[16] M. Guo, J. Balamurugan, T. D. Thanh, N. H. Kim, J. H. Lee, Facile fabrication of Co_2CuS_4 nanoparticle anchored N-doped graphene for high-performance asymmetric supercapacitors. J. Mater. Chem. A, 4 (2016) 17560-17571.